PROCEEDINGS OF SCIENCE

How does the Beaming Effect Beam the TeV Blazars

Yanjun Qian,[a] **Peizhen Hu,**[a] **Shuochun Wang,**[a] **Hengji Zhang,**[a] **Yubin Lai,**[a] **Jianhong Cao**[a] **and Zhiyuan Pei**[a,b,c,*]

[a] *School of Physics and Materials Science, Guangzhou University, Guangzhou 510006, People's Republic of China*

[b] *Center for Astrophysics, Guangzhou University, Guangzhou 510006, People's Republic of China*

[c] *Astronomy Science and Technology Research Laboratory of Department of Education of Guangdong Province, Guangzhou 510006, People's Republic of China*

E-mail: yanjunqian2024@163.com, peizy@gzhu.edu.cn

The detection of TeV emission in extragalactic galaxies has motivated detailed investigations into the beaming effect in blazars, a defining characteristic of relativistic jets that modulates multi-wavelength radiation, though quantitative constraints remain limited. This study systematically analyzes the beaming effect in TeV blazars by disentangling beamed and unbeamed components in high-energy spectra (X-ray, γ-ray, TeV bands) and estimating Doppler factors across these bands, thereby probing their de-beamed intrinsic luminosities. Utilizing a comprehensive sample of TeV blazars, we apply a two-component model to decompose core-dominated and extended emissions. Doppler factors are derived from core-dominance parameters and jet geometries. Results indicate that low-energy peaked sources (LBLs) sources exhibit the strongest beaming, confirming that high energy core-dominance parameters serve as robust tracers of the beaming effect. Doppler factors peak in the γ-ray band and display a concave-to-convex evolutionary pattern from radio to TeV energies, suggesting distinct emission regions or viewing angles across bands. The derived Doppler factors enable calculation of de-beamed intrinsic luminosities, providing new insights into the intrinsic properties of blazar jets.

39th International Cosmic Ray Conference (ICRC2025)
15–24 July 2025
Geneva, Switzerland

ICRC 2025
The Astroparticle Physics Conference
Geneva July 15-24, 2025

*Speaker

PoS(ICRC2025)801

1. Introduction

Blazars are radio-loud active galactic nuclei (AGNs) characterized by relativistic jets aligned with our line of sight . Their emission is dominated by Doppler-boosted non-thermal radiation from jets, resulting in broadband variability from radio to γ-rays. Key observational features include high polarization, rapid variability, superluminal motion, and strong γ-ray emission [1–3]. Blazars are classified into BL Lac objects (EW$<$ 5 Å) and flat-spectrum radio quasars (FSRQ, EW$\geq$ 5 Å) based on optical emission line strength. Their spectral energy distributions (SEDs) exhibit two broad humps: a synchrotron-dominated low-energy peak (IR–X-ray) and an inverse Compton (IC) high-energy peak (MeV–TeV).

Beaming effect plays an important role in the blazar-jet environment that the emission of jets is predominantly influenced by relativistic beaming effect. When a sub-source moves at relativistic velocity, the corresponding Doppler factor, also known as the beaming factor, can be calculated via $\delta = [\Gamma\,(1-\beta\cos\theta)]^{-1}$, where $\Gamma = \left(1-\beta^2\right)^{-\frac{1}{2}}$ ($\beta = \frac{v}{c}$) denotes the Lorentz factor of the jet, θ is the angle between the jet and the observer's line of sight . Among all AGNs, blazars exhibit the smallest radial angle (typically $< 5°$), thus resulting in a large Doppler factor and the strongest beaming effect [4]. Therefore, investigating the beaming effect can provide valuable insights into the nature of blazars and contribute to our understanding of the evolution of AGN.

Over the past two decades, TeV astronomy has matured into a well-established discipline, expanding from initial detections of few sources to current catalogs of 84 TeV blazars detected by Imaging Atmospheric Cherenkov Telescopes(IACTs). These observations have significantly advanced our understanding of high-energy astrophysics and astroparticle physics . Multiwavelength studies reveal correlated GeV/TeV variability and distinct spectral properties between TeV-detected and non-detected BL Lacs , further motivating focused investigation.

Since blazars occupy the majority of TeV AGNs, thus we believe the beaming effect in TeV blazars is worth researching that paving us a new way to explore the VHE mechanism.However, direct measurement of δ in high-energy bands (X-ray to TeV) remains challenging due to undetectable viewing angles. To address this limitation, we develop a novel methodology for estimating Doppler factors specifically in X-ray, γ-ray, and TeV bands for TeV-detected blazars.

2. Method

2.1 High-Energy Core-Dominance

Thanks to the great contributions by the Very Large Array (VLA)[1] and Very Long Baseline Interferometry observations (VLBI)[2], the two-component model decomposes total radio luminosity ($L_{\rm obs}$) into beamed ($L_{\rm core}$) and unbeamed ($L_{\rm ext}$) components, i.e., $L_{\rm obs} = L_{\rm core} + L_{\rm ext.}$.The ratio of the two components, $R_{\rm radio} = L_{\rm core}/L_{\rm ext.}$, is defined as the radio core-dominance parameter . Previous works pointed out that $R_{\rm radio}$ can be act one of the beaming factors and are associated with others $(\delta, \Gamma, \beta, \theta)$ [5]

$$R_{\rm radio} = f\Gamma^{-p}\left[(1-\beta\cos\theta)^{-p} + (1+\beta\cos\theta)^{-p}\right], \tag{1}$$

[1] https://public.nrao.edu/telescopes/vla/

[2] https://www.esa.int/Science_Exploration/Space_Science/Observations_Very_Long_Baseline_Interferometry_VLBI

where $f = S^{\rm int}_{\rm core}/S^{\rm int}_{\rm ext.}$ is an intrinsic ratio defined by the intrinsic flux density of the jet to the extended flux density in the co-moving frame, and the value of p depends on the shape of the emitted spectrum and the physical properties of the jet, with $p = 2 + \alpha$ for a continuous jet and $p = 3 + \alpha$ for a moving blob or a sphere (α is the radio spectral index). The first term denotes the jet radiation toward the observer, while the second term represents the jet radiation backwards the observer. When the viewing angle is small (e.g. $\theta < 5°$), the above relation yields,

$$R_{\rm radio} \simeq f\,[\Gamma\,(1-\beta\cos\theta)]^{-p} = f\delta^{p}, \tag{2}$$

thus the radio core-dominance parameter can play a key role in beaming effect, and one can use Equation (2) to estimate the Doppler factor if $R_{\rm radio}$ is given. Beside, another crucial parameter could be taken into consideration that signifying the ratio of the luminosity in the jet to the unbeamed luminosity when $\theta = 90°$, i.e., the value of $R_{\rm radio}$ at transverse alignment, namely $R_{\perp{\rm radio}} = R_{\rm radio}(90°)$, then the radio core dominance parameter for a source, are constrained in the range from $R_{\perp{\rm radio}}$ to $R_{\perp{\rm radio}}\Gamma^2(2\Gamma^2-1)$. $R_{\perp{\rm radio}}$ can also be calculated via $R_{\perp{\rm radio}} = \frac{2f}{\Gamma^p}$ [5], therefore one can read

$$R_{\rm radio} = R_{\perp{\rm radio}}\frac{1}{2}\left[(1-\beta\cos\theta)^{-p} + (1+\beta\cos\theta)^{-p}\right]. \tag{3}$$

Orr & Browne (1982)[9] firstly obtained an estimate of $R_{\perp{\rm radio}} = 0.024$ at 5 GHz based on a selected-sample of 32 randomly orientated FSRQs. We also proposed that $R_{\perp{\rm radio}}$ is a perhaps better parameter than the well-known radio core dominance parameter $R_{\rm radio}$ to reveal more intrinsic physical properties between BL Lacs and FSRQs.

However for X-ray, γ-ray, and TeV bands where direct component separation is infeasible, we compute the superluminal motion parameter $\beta\cos\theta$ from radio data [6, 7]:

$$\beta\cos\theta = \left\{\frac{2R_{\rm radio} + R_{\perp{\rm radio}} - \left[R_{\perp{\rm radio}}(8R_{\rm radio} + R_{\perp{\rm radio}})\right]^{1/2}}{2R_{\rm radio}}\right\}^{1/2}. \tag{4}$$

Assuming band-independent $\beta\cos\theta$, the core-dominance parameter in band i is:

$$R_i = R_{\perp i}\cdot g_i(\beta,\cos\theta), \tag{5}$$

where

$$g_i = \frac{1}{2}\left[(1-\beta\cos\theta)^{-(2+\alpha_i)} + (1+\beta\cos\theta)^{-(2+\alpha_i)}\right]. \tag{6}$$

The couple beaming factor $g_i(\beta,\cos\theta)$ can be obtained using $\beta\cos\theta$ solved from Equation (5), and $R_{\perp i}$ should be considered as a constant and can be determined by minimizing the observed radiation against the beamed radio core emission in each band, respectively. Finally, we can derive R_i using Equation (6) when $R_{\perp i}$ is determined.

2.2 Spectral Index Separation

High and variable polarization is one of the most prominent characteristics of blazars, which is believed to be associated with the beaming effect. Our previous study pointed out that the radio core-dominance parameter has been related with the polarization in radio band [10],

$$\alpha_{\rm total} = \frac{R_{\rm radio}}{1+R_{\rm radio}}\alpha_{\rm beamed} + \frac{1}{1+R_{\rm radio}}\alpha_{\rm unbeamed}, \tag{7}$$

The above idea can be employed in the high energy band if we assume the spectral index (or photon index) is also constituted by the beamed and unbeamed contribution. In this sense, Equation (7) can be extended to

$$\alpha^i_{\rm total} = \frac{R_i}{1+R_i}\alpha^i_{\rm beamed} + \frac{1}{1+R_i}\alpha^i_{\rm unbeamed} \tag{8}$$

2.3 Doppler Factor Estimation

Extending Equation (2) to high-energy bands, one can obtain

$$R_i = f_i \delta_i^p \quad (i = {\rm X}, \gamma, {\rm TeV}), \tag{9}$$

where $p = 2+\alpha_i$ (continuous jet) or $3+\alpha_i$ (spherical blob). Using radio Doppler factors $\delta_{\rm radio}$ from literature and:

$$\Gamma^p = \frac{2 f_i}{R_{\perp i}}, \tag{10}$$

We assume the value of $\Gamma_{\rm radio}$ obtained in the radio band are universal and can be applied to other wavelengths, so that we can compute band-specific Doppler factors $\delta_i = (R_i/f_i)^{1/p}$ [8].

2.4 De-beamed Luminosity Calculation

Intrinsic (de-beamed) luminosities are:

$$L_i^{\rm in} = L_i^{\rm obs}/\delta_i^{3+\alpha_i} \quad \text{(continuous jet)} \tag{11}$$

$$L_i^{\rm in} = L_i^{\rm obs}/\delta_i^{4+\alpha_i} \quad \text{(spherical blob)}, \tag{12}$$

with K-corrected observed luminosities:

$$L_\gamma^{\rm obs} = 4\pi d_{\rm L}^2 (1+z)^{\alpha_\gamma^{\rm ph}-2} F_\gamma \tag{13}$$

$$L_{\rm TeV} = 4\pi d_{\rm L}^2 (1+z)^{\alpha_{\rm TeV}^{\rm ph}-2} F_{\rm TeV} \tag{14}$$

3. Result and Discussion

3.1 Multiwavelength Core-Dominance Parameters

The distributions of the multiwavelength core-dominance parameters for TeV blazars is shown in Figure 1. We classify our sample into there groups, HBL/IBL/FSRQ+LBL, which are labeled in the red-shaded areas, green-shaded areas and blue-shaded areas, respectively. A clear tendency that a downward trend in the peak value as the core-dominance parameter increases is firstly catching our eye. This trend can be interpreted as a decrease in the viewing angle, indicating an enhanced beaming effect and an increased Doppler factor.

The first distribution refers to the radio core-dominance parameters, $\log R_{\rm radio}$. The average value for 31 HBLs is $< \log R_{\rm radio} >= 0.50 \pm 0.89$ with a median of 0.16. The peak of probability density is beyond half ($\rho = 0.52$), situating at $\log R_{\rm radio} = 0.11$. On the other hand, the peak for 13 IBLs is placed in $\log R_{\rm radio} = 0.53$ with a distribution density $\rho = 0.34$, and also has an obtuse peak located in $\log R_{\rm radio} = 2.13$ with $\rho = 0.26$. The average value for IBLs sample is $< \log R_{\rm radio} >= 1.28 \pm 0.98$ and hold a median of 0.97. Lastly, for 7 FSRQs+LBLs sample,

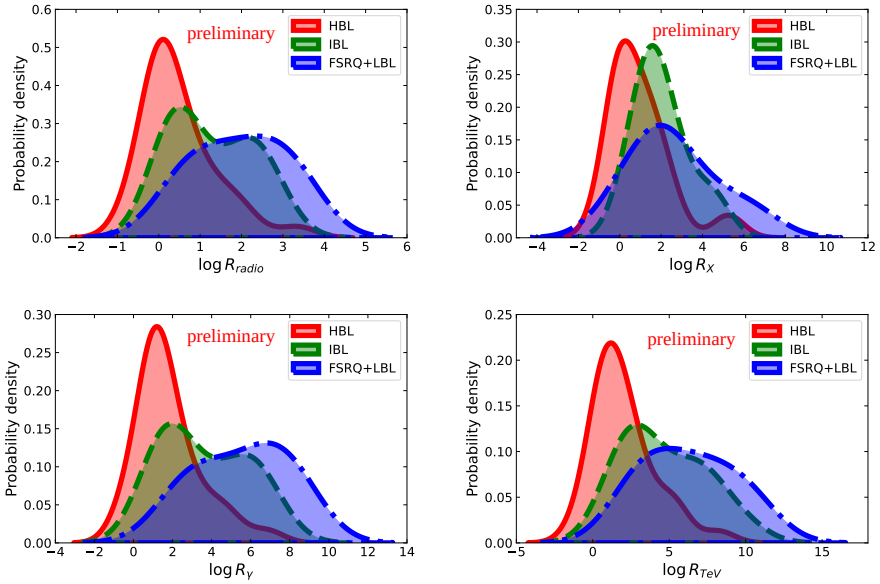

Figure 1: Distributions of core-dominance parameters for radio, X-ray, γ-ray and TeV emission. The red-shaded region refers to high synchrotron peak, or high-energy BL Lacs (HBLs), the green one denotes the intermediate BL Lacs (IBLs), and the blue one signifies the group combined with low BL Lacs (LBLs) and FSRQs. All the values of core-dominance parameters are in logarithm.[8].

on average we obtain $<\log R_{\rm radio}>= 1.96 \pm 1.12$. The median is 2.16, which is rather close to the average value, making the distribution is quite placid. The distribution peak situates in $\log R_{\rm radio} = 2.38$ with a density $\rho = 0.27$. The density peak appears that the low-energy synchrotron peak TeV sources are lying broadly in the range of larger radio core-dominance parameters, while the high-energy synchrotron peak TeV sources are holding the less radio core-dominance parameters. This implies that TeV FSRQs or TeV IBLs have a stronger beaming effect than that of TeV HBLs and TeV IBLs in the radio band, or the viewing angles within former are on average smaller than latter.

The derived X-ray core-dominance parameters distributions are shown in the second panel. Notably, HBLs and IBLs both possess a sharp peak with comparable probability density at nearby $\rho \simeq 0.30$ in where $\log R_x = 0.27$ and $\log R_x = 1.58$, respectively. Meanwhile, HBLs also peaks in $\log R_x = 5.24$ with density $\rho = 0.03$. The average value and median of HBLs, $<\log R_x>= 0.98 \pm 1.47$ and 0.65, are obtained. The IBLs subclass in this case exhibit a more concentrated distribution compared with the radio emission behavior, with $\log R_x$ value ranging from 0.10 to 4.80 and an average value of $<\log R_x>= 2.03 \pm 1.32$ with a median of 1.76. For FSRQs+LBLs, $\log R_x$ spans from -0.02 to 6.37, with an average value of $<\log R_x>= 2.66 \pm 2.12$. Similar to $\log R_{\rm radio}$, this subgroup show a wide region and overlap the other two subsamples. Interestingly, at a distribution density of $\rho = 0.17$, FSRQ+LBLs peaks in $\log R_x = 1.96$, verging on the peak of IBLs.

The third panel displays the distribution of the γ-ray core-dominance parameters for three groups. HBLs sample likewise take up a protruding peak in $\log R_\gamma = 1.21$ at a probability density of $\rho = 0.28$. The average value and median is $<\log R_\gamma>= 1.82 \pm 1.65$ and 1.31, separately. The

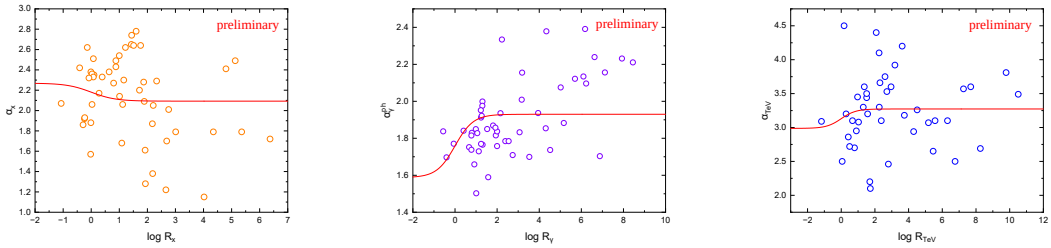

Figure 2: Plot of the correlation that the spectral index against core- dominance parameter in each band.[8].

subgroup of IBLs in this case show two peaks. The first one is at $\log R_\gamma = 2.01$ ($\rho = 0.16$) and another at $\log R_\gamma = 5.56$ ($\rho = 0.12$). We find their average is $< \log R_\gamma >= 3.63 \pm 2.16$ and the median is 3.17. Lastly, $< \log R_\gamma >= 5.56 \pm 2.37$ and median of 6.18 are reached for FSRQs and LBLs. They peak in $< \log R_\gamma >= 6.76$ with $\rho = 0.13$. The distributivity of this parameter is quite similar with $\log R_{\rm radio}$. Two shapes are nearly the same only differ in the magnitude of $\log R_\gamma$ is enlarging, which indicates (1) the radio emission and γ-ray emission is closely correlative; (2) the γ-ray emission originating within the TeV blazars jets are perhaps stronger beamed than the radio emission

The last panel describes the distributions of TeV core-dominance parameters for three groups. The FSRQs+IBLs subclass has $\log R_{\rm TeV}$ values ranging from 2.6 to 10.51 with an average value of $< \log R_{\rm TeV} >= 6.24 \pm 2.96$. On the other hand, the IBLs subgroup exhibits $\log R_{\rm TeV}$ values scoping from 21.51 to 9.79, with an average value of $< \log R_{\rm TeV} >= 4.67 \pm 2.67$. For the HBLs, the $\log R_{\rm TeV}$ values range from -1.17 to 8.26 with an average value of $\log R_{\rm TeV}$ are $< \log R_{\rm TeV} >= 2.11 \pm 2.02$. The medians of distributions are 1.61, 3.62 and 6.31, separately. These values are over treble larger than that in the radio band and marginally higher than that in the γ-ray emission. The probability density of three subsample peaks in $\log R_{\rm TeV} = 1.19$ ($\rho = 0.22$) for HBLs, $\log R_{\rm TeV} = 2.92$ ($\rho = 0.13$) for IBLs, and $\log R_{\rm TeV} = 5.03$ ($\rho = 0.10$) for LBLs, showing that the range of core dominance of the TeV luminosity is rather radical.

3.2 Correlation Between Core-Dominance Parameters and Spectral Indices

Now we adopt Equation (8) across our present TeV sample, and the fitting demonstrations are shown in Figure (2). The panels from left to right hand side are the X-ray photon index against X-ray core-dominance parameter, γ-ray photon index against γ-ray core-dominance parameter, and TeV spectral index against TeV core-dominance parameter, respectively. The core index and extended spectral index can be determined by minimizing $\Sigma \left[\alpha^i_{\rm total} - \alpha^i_{\rm beamed} R_i/(1+R_i) + \alpha^i_{\rm unbeamed}(1+R_i)\right]^2$.

The above relation unmasks a truth that the total spectral index in high energy band is also composed by two components since the high energy emissions are also strong beamed, namely the core/beamed and extended/unbeamed parts. By adopting the correlation between the spectral indices (or photon indices) and core-dominance parameters from the radio band to TeV emission, we conclude that the total observed spectral indices are mainly coming from the beamed or jet component. This finding supports the validity of the two-component emission model in TeV blazars

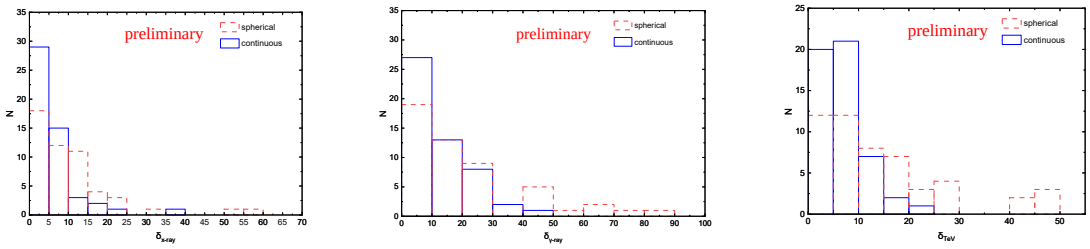

Figure 3: Distributions of estimated Doppler factors in X-ray, γ-ray and TeV band. The red-dashed line and blue-solid line refer to the scenario of spherical and continuous jet respectively, corresponding to $p = 3 + \alpha^i$ and $2 + \alpha^i$, where α^i is the spectral index in X-ray, γ-ray and TeV band[8].

3.3 Doppler Factors

Employing the method we present, we can estimate the Doppler factors in high energy band, and the derived results are demonstrated in Figure 3. The histogram illustrates the statistical distribution of Doppler factors across X-ray, γ-ray and TeV bands, comparing the fits between spherical and continuous geometric models. In the X-ray band, the Doppler factor mainly distributed between 1 and 40. The median values are $\delta_{\rm X} = 14.17$ (continuous) and $\delta_{\rm X} = 9.06$ (spherical), respectively. In the γ-ray, the δ_γ distribution for the continuous model spans $1 \sim 80$, with medians of $\delta_\gamma = 26.79$ (continuous) and $\delta_\gamma = 19.62$ (spherical). Since the radio Doppler factors on average usually fall in the range of $15 \sim 30$, thus our derived γ-ray Doppler factors exhibit similar characteristics with ones in radio band. This can be deemed to another evidence that γ-ray and radio emission is tightly correlative in γ-loud blazars, and also perhaps in TeV blazars. In contrast, TeV Doppler factors are narrowly distributed from 1 to 35, with medians of $\delta_{\rm TeV} = 12.73$ (continuous) and 9.89 (spherical). The lower TeV values may originate from unique radiative processes or severe γ absorption limiting high-δ detections. These results underscore the energy-dependent nature of Doppler boosting and emphasize the necessity of band-specific radiative and geometric models in blazar studies.

Our δ-derived result shows a concave from radio to X-ray while a convex from X-ray to TeV emission, and $\delta_{\rm radio} \approx \delta_\gamma$ for both $2 + \alpha_i$ or $3 + \alpha_i$, indicating (i) the γ-ray and radio emission are co-spatial within blazar's jet; (ii) the TeV and X-ray emission region are closer to the central black hole. However, the varied δ_i may also be due to the different θ_i in each band, thus our result also reveals that (iii) the diminishing tendency from radio to X-ray and γ-ray to TeV band implies the jets change the angles with respect to the line of sight (getting smaller), and the raising tendency from X-ray to γ-ray requires the jets' angles becoming larger [8].

4. Summary

This work is under review now. All the results and figures we display here are preliminary. In this study, we delve into the beaming effect and physical mechanism governing multiwavelength emission from the TeV-detected blazars. Our approach involved constructing a comprehensive dataset of large sample of TeV blazars, encompassing one of key indicators for beaming, namely core-dominance parameters from the radio to TeV band. Utilizing an analytical framework, we successfully implemented a two-component model to unravel the unique TeV emission signatures of

these objects. Additionally, we performed a rigorous analysis of the correlations among multiwavelength luminosity, emission core dominance, and spectral index across distinct blazar subclasses. Our salient conclusions are as follows:

1. Overall, our results reveal that FSRQ+LBL sources exhibit a broadest distribution of core-dominance parameters, and generally take on the higher value range, indicating the low-energy or low-synchrotron peak blazars possess stronger beaming regardless of their frequency bands. Collectively, we demonstrate the multiwavelength emission within our compiled TeV sources are beamed, and hence, the core-dominance parameters in high energy bands can also act the indicators for beaming effect.

2. The predominance of the beamed or jet component in shaping the observed total spectral index in the high-energy band underscores the applicability of the two-component emission model to TeV blazars, which encapsulates both beamed and unbeamed contributions. Our finding points out the total observed emissions are mainly originated from the core or jet component.

3. We estimate the Doppler factors at high-energy bands for both scenarios of continues and spherical jet launching in TeV blazars. For the case of continues jet, we obtain the median values are $\delta_{\rm X} = 14.17$, $\delta_{\gamma} = 26.79$ and $\delta_{\rm TeV} = 12.73$. On the other hand, $\delta_{\rm X} = 9.06$, $\delta_{\gamma} = 19.62$ and $\delta_{\rm TeV} = 9.89$ are ascertained for spherical blob, respectively. Our results suggest that the universality of beaming effect across diverse wavelength bands. We also find a concave from the radio to X-ray while a convex from X-ray to TeV bands, i.e., the Doppler factor is a function of frequency for TeV-detected blazars. This tendency indicates that the emissions at different bands are produced in different emission regions and/or in the same emission region with a different viewing angle.

References

[1] Urry C. M., Padovani P., 1995, PASP, 107, 803

[2] Romero G. E., Cellone S. A., Combi J. A., Andruchow I., 2002, A&A, 390, 431

[3] Fan J., Yang J. H., Zhang J.-Y., Hua T. X., Liu Y., Qin Y.-P., Huang Y., 2013, PASJ, 65, 25

[4] Pei Z., Fan J., Bastieri D., Yang J., Xiao H., 2020, Science China Physics, Mechanics, and Astronomy, 63, 259511

[5] Pei Z., Fan J., Yang J., Bastieri D., 2020, PASP, 132, 114102

[6] Zeng X., Zhang Z., Pei Z., Xiao H., Fan J., 2022, ApSS, 367, 36

[7] Zhang Z., Zeng X., Pei Z., Xiao H., Ye X., Fan J., 2022, PASP, 134, 064101

[8] Qian Yanjun, Pei Zhiyuan, et al. 2025, under review,

[9] Orr M. J. L., Browne I. W. A., 1982, MNRAS, 200, 1067

[10] Fan J.-H., Yang J.-H., Pan J., Hua T.-X., 2011, Research in Astronomy and Astrophysics, 11, 1413